

Least-squares Smoothed Shape Functions for Constructing Field-Consistent Timoshenko Beam Elements

Wong, F.T.^{1*}, Tjahyono, H.G.², Hartono, S.², and Setiabudi, T.A.²

¹ Associate Professor, Department of Civil Engineering, Petra Christian University
Jl. Siwalankerto 121-131, Surabaya 60236, INDONESIA

² Alumnus, Department of Civil Engineering, Petra Christian University
Jl. Siwalankerto 121-131, Surabaya 60236, INDONESIA

DOI: <https://doi.org/10.9744/ced.27.1.22-32>

Article Info:

Submitted: Jan 18, 2025

Reviewed: Feb 04, 2025

Accepted: Mar 01, 2025

Keywords:

Timoshenko beam element,
field consistency,
least-squares smoothed shape function,
shear locking,
bifurcation buckling,
free vibration.

Corresponding Author:

Wong, F.T.

Department of Civil Engineering,
Petra Christian University
Jl. Siwalankerto 121-131, Surabaya
60236, INDONESIA
Email: wftjong@petra.ac.id

Abstract

This paper presents an approach for constructing field-consistent Timoshenko beam elements using least-squares smoothed (LSS) shape functions. The variational basis for shear strain redistribution is thoroughly explained, leading to the derivation of LSS shape functions for linear, quadratic, and cubic Timoshenko beam elements. These elements are then applied to linear static analysis, bifurcation buckling analysis, and free vibration analysis of prismatic and tapered beams. Numerical tests demonstrate that the LSS-based beam elements effectively eliminate shear locking and provide accurate, reliable results. Their performance is comparable to the discrete shear gap technique but with a simpler implementation procedure. The LSS shape function approach offers a practical and efficient alternative for achieving field consistency in Timoshenko beam elements, with potential applications in enhanced finite element methods (FEMs) such as isogeometric FEM and Kriging-based FEM.

This is an open access article under the [CC BY](https://creativecommons.org/licenses/by/4.0/) license.



INTRODUCTION

Beam finite elements are essential in practical structural engineering applications. One of the most widely used theories for developing beam elements is the Timoshenko beam model [1], which accounts for shear deformation and cross-sectional rotatory inertia. However, Timoshenko beam elements developed strictly from the standard displacement-based finite element formulation can produce erroneous results, particularly in the case of thin beams. These errors may manifest as very small displacement results compared to the correct solution—a phenomenon known as shear locking [2]—as well as suboptimal convergence or severe oscillations in the shear force distribution [3,4].

The primary cause of these errors is that the standard finite element formulation, which employs the same interpolation scheme for both deflection and rotation fields, leads to an inconsistent transverse shear strain field [3]. This means that the approximate shear strain is inconsistent with the physical behavior of thin beams, where the shear strain approaches zero. Thus, standard Timoshenko beam elements are unable to represent bending deformation without transverse shear strain (shearless bending deformation).

An early proposed method to make Timoshenko beam elements consistent and hence free from shear locking is the selective reduced integration (SRI) technique [2]. In this technique, the number of Gaussian quadrature sampling points for evaluating the stiffness matrix associated with shear deformation is intentionally reduced from the one

Note : Discussion is expected before July, 1st 2025, and will be published in the "Civil Engineering Dimension", volume 27, number 2, September 2025.

ISSN : 1410-9530 print / 1979-570X online

Published by : Petra Christian University

required for an exact integration. This technique has also been applied in various enhanced finite element methods (FEMs), including Kriging-based FEM [5] and NURBS (Non-Uniform Rational B-Splines) isogeometric FEM [6]. The SRI technique can effectively eliminate the shear-locking phenomenon in both traditional and enhanced FEMs. However, the resulting shear force is only accurate at the quadrature sampling points. The overall shear force distribution can be even more erratic (oscillating) than that of the original inconsistent beam element [4,5].

A more recent method to ensure consistency in Timoshenko beam elements and eliminate shear locking is the discrete shear gap (DSG) technique [7]. In this technique, the inconsistent shear strain field is replaced with a substitute shear strain field derived from the interpolated shear gap. Wong and Sugianto [8] demonstrated that the DSG technique is effective in ensuring the consistency of linear, quadratic, and cubic Timoshenko beam elements. Furthermore, this technique has also been successfully applied within the frameworks of Kriging-based FEM [9-12] and NURBS isogeometric FEM [6,13]. Although the DSG technique works perfectly to make Timoshenko beam elements consistent, its implementation procedure is quite complicated.

A simpler alternative method for achieving field consistency in Timoshenko beam elements is to redistribute the shear strain field using a set of least-squares smoothed (LSS) shape functions for the rotation field. This approach was originally proposed by Prathap and Babu [14-16] for eliminating shear locking and/or membrane locking in shear-deformable linear and quadratic beams. However, this simple strain redistribution technique does not appear to be widely recognized (outside Prathap and co-workers' research group), which can be attributed to several reasons. The LSS shape functions in References [14-16] were presented without a derivation, and there was no detailed elaboration on the variational principle associated with the strain redistribution.

This paper aims to present in detail the variational basis for the redistribution of shear strain and outline a systematic procedure for constructing LSS shape functions in Timoshenko beam elements. The procedure is used to develop a set of LSS shape functions for linear, quadratic, and cubic Timoshenko beam elements. The resulting beam elements are then applied for linear static analysis, bifurcation buckling analysis, and free vibration analysis of prismatic or tapered beams. A series of numerical tests are conducted to evaluate the performance of these field-consistent beam elements. The results are compared to those obtained using the original field-inconsistent beam elements and the beam elements with the DSG technique [8].

Timoshenko Beam Elements

Governing Variational Equations

Consider a beam of length L that is subjected to a distributed transverse load $q = q(X, t)$ and an axial compressive load $P = P(t)$, as illustrated in Figure 1. The beam is assumed to be made from a homogeneous and isotropic linear elastic material with a modulus of elasticity E , shear modulus G , and mass density ρ . According to Timoshenko beam theory, the motion of the beam at any time $t \geq 0$ can be described using two independent field variables: the deflection of the neutral axis $w = w(X, t)$ and the rotation of cross sections $\theta = \theta(X, t)$, $0 \leq X \leq L$.

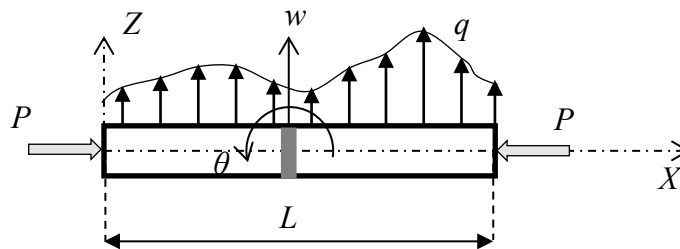


Figure 1. Coordinate System and the Positive Sign Convention for the Beam Deflection, w , Cross-Section Rotation θ , Distributed Load q , and Axial Load P

The weak form of governing equations for the beam motion that accounts for the effect of the axial force on bending deformation can be written as [9]:

$$\int_0^L \delta w \rho A \ddot{w} dX + \int_0^L \delta \theta \rho I_Y \ddot{\theta} dX + \int_0^L \delta \theta_{,X} E I_Y \theta_{,X} dX + \int_0^L \delta \gamma k G A \gamma dX - \int_0^L \delta w_{,X} P w_{,X} dX = \int_0^L \delta w q dX, \tag{1}$$

for all $\delta w \in \mathbb{H}^1(0, L)$ and for all $\delta \theta \in \mathbb{H}^1(0, L)$

In this equation, the symbol δ denotes the variational operator; A and I_Y denote the cross-sectional area and the cross-sectional second moment of area about the Y -axis, respectively. In general, A and I_Y may vary along the length of the beam. The variable k refers to the shear correction factor, which depends on the geometrical shape of the beam. The double dots signify the partial second derivative of the corresponding variable with respect to time t , whereas the comma followed by subscript X signifies the partial derivative of the variable with respect to X . The shear strain γ is given as

$$\gamma = w_{,X} - \theta \tag{2}$$

The symbol $\mathbb{H}^1(0, L)$ denotes the Sobolev function space of the first degree in interval $0 < X < L$.

The bending moment and the shear force (perpendicular to the X -axis) are given as [9]:

$$M = EI_Y \theta_{,X} \tag{3}$$

$$Q = kGA(w_{,X} - \theta) - Pw_{,X} \tag{4}$$

Finite Element Formulation

Suppose the beam is partitioned into N_e number of elements with N_p number of nodes. Consider a typical beam element (element number e) possessing n nodes. The displacement and rotation fields over this element are approximated as follows:

$$w \approx w^h = \sum_{i=1}^n N_i(\xi) w_i(t) = [N_w]\{d\} \tag{5}$$

$$\theta \approx \theta^h = \sum_{i=1}^n N_i(\xi) \theta_i(t) = [N_\theta]\{d\} \tag{6}$$

$$[N_w] = \{N_1(\xi) \quad 0 \quad N_2(\xi) \quad 0 \quad \dots \quad N_n(\xi) \quad 0\} \tag{7}$$

$$[N_\theta] = \{0 \quad N_1(\xi) \quad 0 \quad N_2(\xi) \quad \dots \quad 0 \quad N_n(\xi)\} \tag{8}$$

$$\{d\} = \{w_1(t) \quad \theta_1(t) \quad w_2(t) \quad \theta_2(t) \quad \dots \quad w_n(t) \quad \theta_n(t)\}^T \tag{9}$$

In these equations, the superscript h refers to the association of w^h and θ^h with a discretization using a mesh of an element characteristic length scale h . Function $N_i(\xi)$ represents the element shape functions associated with node i ; $w_i(t)$ and $\theta_i(t)$ represent the deflection and rotation at nodal point number i , respectively. The shape functions are expressed in terms of natural coordinate ξ , $-1 \leq \xi \leq 1$.

The shape functions for a two-node linear element, a three-node quadratic element, and a four-node cubic element are respectively given as (assuming nodes 1 and 2 are the end nodes and the rests are the interior nodes):

$$N_1 = \frac{1}{2}(1 - \xi), \quad N_2 = \frac{1}{2}(1 + \xi) \tag{10}$$

$$N_1 = -\frac{1}{2}\xi(1 - \xi), \quad N_3 = 1 - \xi^2, \quad N_2 = \frac{1}{2}\xi(1 + \xi) \tag{11}$$

$$N_1 = -\frac{1}{16}(1 - \xi)(1 - 9\xi^2), \quad N_3 = \frac{9}{16}(1 - 3\xi)(1 - \xi^2),$$

$$N_4 = \frac{9}{16}(1 + 3\xi)(1 - \xi^2), \quad N_2 = -\frac{1}{16}(1 + \xi)(1 - 9\xi^2) \tag{12}$$

The mapping from natural coordinate ξ to the global coordinate X is given as

$$X = \sum_{i=1}^n N_i(\xi) X_i; \quad J = X_{,\xi} \tag{13}$$

In this equation, X_i is the global coordinate of nodal point number i and J is the Jacobian of the mapping.

To derive the finite element equations, the integrals in the variational equation, Equation (1), are firstly expressed as the sum of the integrals over each element interval. Subsequently, substituting Equations (5) and (6) into the resulting equation and applying the standard finite element formulation yield the discretized system of equations as follows:

$$[M]\{\ddot{D}(t)\} + ([K] - P[K_g])\{D(t)\} = \{F(t)\} \tag{14}$$

where $[M]$, $[K]$, $[K_g]$ are the discretized structural mass, stiffness, and geometric stiffness matrices, respectively. The vector $\{D(t)\}$ is the vector of global nodal displacement, that is,

$$\{D(t)\} = [w_1(t) \quad \theta_1(t) \quad w_2(t) \quad \theta_2(t) \quad \dots \quad w_{N_p}(t) \quad \theta_{N_p}(t)]^T \tag{15}$$

The vector $\{F(t)\}$ is the vector of global nodal force.

The structural mass, stiffness, and geometric stiffness matrices, as well as the global nodal force vector, are obtained by assembling the element mass matrix, $[m]^e$, the element stiffness matrix, $[k]^e$, the element geometric stiffness matrix, $[k_g]^e$, and the element nodal force vector, $\{f\}^e$, respectively, for all elements (i.e., element number $e = 1$ to N_e). These element matrices are defined as follows:

$$[m]^e = \int_{-1}^1 [N_w]^T \rho A [N_w] J d\xi + \int_{-1}^1 [N_\theta]^T \rho I_Y [N_\theta] J d\xi \quad (16)$$

$$[k]^e = [k]_b^e + [k]_s^e \quad (17a)$$

$$[k]_b^e = \int_{-1}^1 [N_\theta]_{,\xi}^T EI_Y [N_\theta]_{,\xi} J^{-1} d\xi \quad (17b)$$

$$[k]_s^e = \int_{-1}^1 ([N_w]_{,\xi} J^{-1} - [N_\theta])^T kGA ([N_w]_{,\xi} J^{-1} - [N_\theta]) J d\xi \quad (17c)$$

$$[k_g]^e = \int_{-1}^1 [N_w]_{,\xi}^T [N_w]_{,\xi} J^{-1} d\xi \quad (18)$$

The element nodal force vector is defined as

$$\{f\}^e = \int_{-1}^1 [N_w]^T q J d\xi \quad (19)$$

The discretized equations for linear static, free vibration, and bifurcation buckling problems can be derived from Equation (14) by reducing it, respectively, to

$$[K]\{D\} = \{F\} \quad (20)$$

$$[M]\{\ddot{D}(t)\} + [K]\{D(t)\} = \{0\} \quad (21)$$

$$([K] - P[K_g])\{D\} = \{0\} \quad (22)$$

Least Squares Smoothed Shape Functions

As mentioned in the introduction section, the standard interpolations for the Timoshenko beam field variables, i.e. Equations (5) and (6), result in a discretized shear strain, γ^h , that is inconsistent with the physical constraint of vanishing the shear strain, Equation (2), when the beam becomes infinitely thin (the Kirchhoff constraint). This inconsistency in the discretized shear strain leads to shear locking, poor convergence, and severe stress oscillation commonly observed when using standard displacement-based Timoshenko beam elements [3] (with exact calculation of all integrals).

To develop beam elements that are consistent with the Kirchhoff constraint, Prathap and Babu [14-16] proposed a set of least-squares smoothed shape functions for interpolating the rotation field in the shear strain expression. This section addresses the variational basis and a detailed derivation of the smoothed shape functions.

Variational Basis

The variational basis for the development of a field-consistent Timoshenko beam element is a modified Hellinger-Reissner's variational principle [3,17]. In this principle, the discretized strain energy for a Timoshenko beam element of length L^e is expressed in the following form:

$$U^h = \int_0^{L^e} \frac{1}{2} EI_Y (\theta_{,x}^h)^2 dx - \int_0^{L^e} \frac{1}{2} kGA \bar{\gamma}^2 dx + \int_0^{L^e} kGA \bar{\gamma} \gamma^h dx \quad (23)$$

where θ^h and γ^h are the discretized rotation and the discretized kinematic shear strain, respectively, while $\bar{\gamma}$ denotes an assumed shear strain. The variable x is the element coordinate, starting from the left end of the beam element. A variation of the functional in Equation (23) with respect to $\bar{\gamma}$ yields

$$\int_0^{L^e} \delta \bar{\gamma} kGA (\gamma^h - \bar{\gamma}) dx = 0 \quad (24a)$$

For a prismatic beam element made from a homogeneous material, kGA is constant along the element, hence Equation (24a) simplifies to

$$\int_0^{L^e} \delta \bar{\gamma} (\gamma^h - \bar{\gamma}) dx = 0 \quad (24b)$$

Equation (24) is known as the orthogonality condition [3]. This orthogonality condition can be utilized to determine a consistent assumed shear strain field, $\bar{\gamma}$, from the already known kinematically derived inconsistent γ^h .

Least Squares Smoothed Shape Functions

A method to achieve consistency in the shear strain field is to redistribute the kinematic shear strain through a least-squares smoothing approach [14,16]. This process begins by defining the assumed shear strain field and its variations as follows:

$$\bar{\gamma} = w_{,x}^h - \bar{\theta} \tag{25a}$$

$$\delta \bar{\gamma} = -\delta \bar{\theta} \tag{25b}$$

where $\bar{\theta}$ is the unknown substitute rotation field. Substituting these equations into Equation (24b) results in

$$\int_0^{L^e} \delta \bar{\theta} (\theta^h - \bar{\theta}) dx = 0 \tag{26}$$

This equation can be interpreted as the stationary condition of the following functional:

$$F(\bar{\theta}) = \int_0^{L^e} \frac{1}{2} (\theta^h - \bar{\theta})^2 dx \tag{27}$$

Thus, the orthogonality condition of the rotation, expressed in Equation (26), requires that the substitute rotation field, $\bar{\theta}$, is a least-squares equivalent of the discretized rotation field, θ^h .

Next, the substitute rotation field is defined as follows:

$$\bar{\theta} = \sum_{i=1}^n \bar{N}_i(\xi) \theta_i(t) = [\bar{N}_\theta] \{d\} \tag{28}$$

where $\bar{N}_i(\xi)$, $i = 1, \dots, n$, represent substitute shape functions. Substituting Equations (6) and (28) into Equation (27) gives

$$F([\bar{N}_\theta]) = \frac{1}{2} \{d\}^T \left[\int_0^{L^e} ([N_\theta] - [\bar{N}_\theta])^T ([N_\theta] - [\bar{N}_\theta]) dx \right] \{d\} \tag{29}$$

This equation indicates that the least-squares substitute rotation field can be obtained by using the least-squares substitute shape functions. Furthermore, to achieve field consistency, these shape functions must be chosen to be a one-order lower polynomial than the order of the shape functions for approximating the deflection. These consistent shape functions are referred to as LSS shape functions.

An example of algebraic calculation for obtaining the LSS shape functions for a quadratic beam element is as follows. The general form of quadratic shape functions is given by:

$$N_i(\xi) = a + b\xi + c\xi^2 \tag{30}$$

The LSS shape functions are chosen to be linear (one degree lower than quadratic), that is,

$$\bar{N}_i(\xi) = \alpha + \beta\xi \tag{31}$$

The coefficients α and β are determined by minimizing the functional:

$$G(\bar{N}_i) = \int_{-1/2}^1 \frac{1}{2} (N_i(\xi) - \bar{N}_i(\xi))^2 d\xi \tag{32}$$

Substituting Equations (30) and (31) into Equation (32) transforms the functional into a function of two variables, α and β , viz.

$$f(\alpha, \beta) = \int_{-1/2}^1 \frac{1}{2} ((a - \alpha) + (b - \beta)\xi + c\xi^2)^2 d\xi \tag{33}$$

The unknown coefficients α and β can be found using the standard calculus method to locate the extreme values of $f(\alpha, \beta)$, that is,

$$\frac{\partial f}{\partial \alpha} = 0 \quad \text{and} \quad \frac{\partial f}{\partial \beta} = 0 \tag{34}$$

Solving these equations yields

$$\alpha = a + \frac{1}{3}c \quad \text{and} \quad \beta = b \quad (35)$$

Thus, the resulting LSS shape function is

$$\bar{N}_i(\xi) = \left(a + \frac{1}{3}c\right) + b\xi \quad (36)$$

Using Equation (36), the LSS shape functions associated with node numbers 1, 2, and 3 for a quadratic beam element can be determined. For instance, the quadratic shape function corresponding to node number 1, refers to Equation (11), has coefficients $a = 0$, $b = -\frac{1}{2}$, $c = \frac{1}{2}$. Substituting these values into Equation (36) yields the LSS shape function associated with node number 1, that is,

$$\bar{N}_1(\xi) = \left(0 + \frac{1}{3}\left(\frac{1}{2}\right)\right) - \frac{1}{2}\xi = \frac{1}{2}\left(\frac{1}{3} - \xi\right) \quad (37)$$

This result is the same as what is presented in Ref. [14,16].

By applying the abovementioned procedure, a set of LSS shape functions for linear, quadratic, and cubic beam elements can be derived. The results are respectively as follows:

$$\bar{N}_1 = \frac{1}{2}, \quad \bar{N}_2 = \frac{1}{2} \quad (38)$$

$$\bar{N}_1 = \frac{1}{2}\left(\frac{1}{3} - \xi\right), \quad \bar{N}_3 = \frac{2}{3}, \quad \bar{N}_2 = \frac{1}{2}\left(\frac{1}{3} + \xi\right) \quad (39)$$

$$\begin{aligned} \bar{N}_1 &= -\frac{1}{16}\left(1 + \frac{22}{5}\xi - 9\xi^2\right), \quad \bar{N}_3 = \frac{9}{16}\left(1 - \frac{6}{5}\xi - \xi^2\right), \\ \bar{N}_4 &= \frac{9}{16}\left(1 + \frac{6}{5}\xi - \xi^2\right), \quad \bar{N}_2 = -\frac{1}{16}\left(1 - \frac{22}{5}\xi - 9\xi^2\right) \end{aligned} \quad (40)$$

The procedure to determine the unknown coefficients in the LSS shape functions described here involves the direct use of the functional, $G(\bar{N}_i)$, as expressed in Eq. (32). Alternatively, the coefficients can be determined by first invoking the stationarity of the functional with respect to \bar{N}_i , which leads to the following equation:

$$\int_{-1}^1 \delta \bar{N}_i(\xi) (N_i(\xi) - \bar{N}_i(\xi)) d\xi = 0 \quad (41)$$

After this, the original shape function and the LSS shape function are substituted into this integral equation. The unknown coefficients in the LSS shape function can then be found by solving the resulting system of linear equations.

It is important to note that, to construct field-consistent Timoshenko beam elements, the LSS shape functions for the rotation field are used to replace the original shape functions solely in the expression corresponding to the shear strain. This specifically applies to the shape functions in the shearing stiffness matrix, as expressed in Equation (17c). Meanwhile, the shape functions for the rotation field in the bending stiffness matrix (Equation (17b)) and the mass matrix (Equation (16)) remain unchanged.

Numerical Tests

The linear, quadratic, and cubic Timoshenko beam elements with the original shape functions (Equations (10), (11), and (12)) and LSS shape functions (Equations (38), (39), and (40)) have been implemented in Matlab. These elements are referred to as ‘Original SF’ and ‘LSS SF’, respectively. They have been tested and applied in static, buckling, and free vibration analyses of prismatic as well as tapered beams. Additionally, for comparison purposes, results obtained using locking-free Timoshenko beam elements with the discrete shear gap technique [8] (referred to as ‘DSG’) are also included in the following report.

The shear modulus and shear correction factor of a beam were calculated using the given modulus of elasticity, E , and Poisson's ratio, ν , with the following formula [18]:

$$G = \frac{E}{2(1+\nu)}, \quad k = \frac{10(1+\nu)}{12+11\nu} \quad (42)$$

Table 1. Minimum Number of Quadrature Sampling Points for Prismatic and Tapered Timoshenko Beam Elements with Original Shape Functions of Different Orders

Element	Mass	Bending Stiffness	Shear Stiffness	Geometry	Force ¹
Prismatic beam					
Linear	2	1	2	1	2
Quadratic	3	2	3	2	2
Cubic	4	3	4	3	3
Tapered beam ²					
Linear	2	1	2	1	2
Quadratic	4	3	3	3	2
Cubic	5	4	4	4	3

¹ Assuming that q is linearly distributed

² The cross-sectional area and moment of inertia are interpolated using the shape functions.

For tapered beams, the cross-sectional area, $A = A(X)$, and moment of inertia, $I_Y = I_Y(X)$, for each beam element are interpolated from their values at the nodes.

The integrals in the element matrix expressions, Equations (16)(19), were evaluated using the Gauss quadrature formula. The minimum number of quadrature sampling points required for each matrix to achieve exact integration results for the beam elements with original shape functions is presented in Table 1. For the beam elements with LSS shape functions, the number of sampling points required to evaluate the shear stiffness matrix can be reduced by one.

Static Analysis

Investigation of Shear Locking

A fixed-fixed supported beam is used to detect shear locking. The geometrical, material, and loading parameters are as follows: $L = 10$ m, $b = 1$ m, $E = 10 \times 10^6$ kN/m², $\nu = 0.3$, and $q = -1$ kN/m. The beam is discretized using eight elements of equal length, as shown in Figure 2. The length-to-thickness ratio of the beam varies from $L/h_B = 5$ (representing a thick beam), to 10, 100, 1000, and 10000 (representing an extremely thin beam). Although a beam with L/h_B greater than 100 is outside the practical range for length-to-thickness ratios, it is included in this test to detect shear locking as the beam becomes extremely thin.

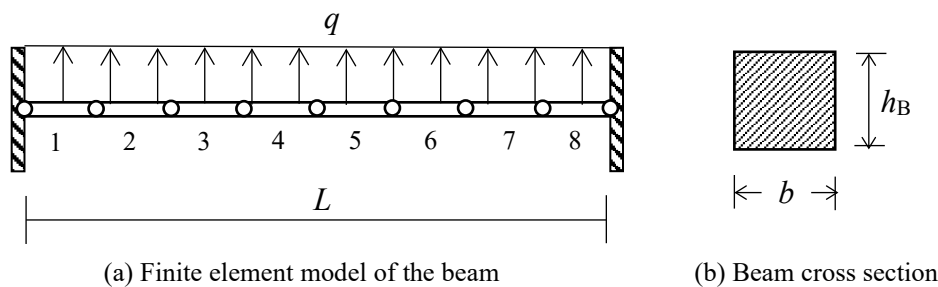


Figure 2. Finite Element Model of a Fixed-Fixed Supported Beam Subjected to a Uniform Load

The analytical solution for the beam mid-span deflection is given by

$$w\left(\frac{L}{2}\right)_{\text{exact}} = \frac{qL^4}{384EI} + \frac{qL^2}{8GkA} \tag{43}$$

The mid-span deflection results obtained using different Timoshenko beam elements, normalized to the exact solution, are presented in Table 2.

The table indicates that the linear, quadratic, and cubic Timoshenko beam elements with the LSS shape functions are free from shear locking. The results are the same as those obtained using beam elements with the DSG technique. In contrast, the linear beam element with the original shape functions experiences shear locking. Although the quadratic original SF element does not suffer from shear locking, it is not as accurate as the quadratic LSS-based element. All cubic beam elements are unaffected by shear locking and can provide exact results for mid-span deflection.

Table 2. Normalized Mid-Span Deflections of a Fixed-Fixed Supported Beam with Different Length-to-Thickness Ratios (L/H_b) Obtained using Various Beam Elements

Element Type	L/h_b				
	5	10	100	1000	1000
Linear Beam Elements					
LSS SF	0.958	0.944	0.938	0.938	0.938
DSG	0.958	0.944	0.938	0.938	0.938
Original SF	0.887	0.662	0.019	0.000	0.000
Quadratic Beam Elements					
LSS SF	1.000	1.000	1.000	1.000	1.000
DSG	1.000	1.000	1.000	1.000	1.000
Original SF	1.000	0.995	0.943	0.938	0.938
Cubic Beam Elements					
LSS SF	All results are exact.				
DSG					
Original SF					

LSS SF: Timoshenko beam elements using the LSS shape functions.

DSG: Timoshenko beam elements with the discrete shear gap technique. The results were taken from Ref. [8].

Original SF: Timoshenko beam elements using the original shape functions.

Assessment of Accuracy and Convergence

To evaluate the accuracy and convergence characteristics of Timoshenko beam elements, the fixed-fixed supported beam with a length-to-thickness ratio of 10 is discretized using different numbers of equal elements: $N_e = 4, 8, 16,$ and 32 . The analysis results for the mid-span deflection, fixed-end moment, and fixed-end shear force, normalized to their corresponding exact values (Equations (43) and (44)), are presented in Tables 3(a)(c).

Table 3. Normalized Mid-Span Deflections, Fixed-End Bending Moments, and Fixed-End Shear Forces of a Fixed-Fixed Supported Beam of $L/H_b = 10$ for Different Number of Elements, N_e , Obtained using Different Beam Elements

(a) Normalized Results using Linear Beam Elements

N_e	Deflection			Bending Moment			Shear Force		
	LSS SF	DSG	Original SF	LSS SF	DSG	Original SF	LSS SF	DSG	Original SF
4	0.777	0.777	0.329	0.375	0.375	0.123	0.750	0.750	1.757
8	0.944	0.944	0.662	0.656	0.656	0.434	0.875	0.875	2.650
16	0.986	0.986	0.887	0.820	0.820	0.727	0.938	0.938	2.423
32	0.997	0.997	0.969	0.908	0.908	0.880	0.969	0.969	1.868

(b) Normalized Results using Quadratic Beam Elements

N_e	Deflection			Bending Moment			Shear Force		
	LSS SF	DSG	Original SF	LSS SF	DSG	Original SF	LSS SF	DSG	Original SF
4	1.000	1.000	0.935	0.938	0.937	0.774	1.000	1.000	2.088
8	1.000	1.000	0.995	0.984	0.984	0.954	1.000	1.000	1.405
16	1.000	1.000	1.000	0.996	0.996	0.992	1.000	1.000	1.117
32	1.000	1.000	1.000	0.999	0.999	0.998	1.000	1.000	1.031

(c) Normalized Results using Cubic Beam Elements

N_e	Deflection			Bending Moment			Shear Force		
	LSS SF	DSG	Original SF	LSS SF	DSG	Original SF	LSS SF	DSG	Original SF
4	All results are exact.			1.000	1.007	0.991	1.000	1.000	1.087
8				1.000	1.002	0.999	1.000	1.000	1.012
16				1.000	1.000	1.000	1.000	1.000	1.002
32				1.000	1.000	1.000	1.000	1.000	1.000

$$M(0)_{\text{exact}} = \frac{1}{12} qL^2, \quad Q(0)_{\text{exact}} = \frac{1}{2} qL \tag{44}$$

Table 3 shows that all results converge to the corresponding analytical values. As expected, higher-order Timoshenko beam elements yield more accurate results compared to lower-order elements. The results of the LSS-based and DSG elements are identical, except for the fixed-end moments obtained from the cubic beam elements, where some minor discrepancies are observed. The performance of the LSS-based element is superior to that of the original SF element.

Moreover, the cubic LSS-based element provides exact results for mid-span deflection, fixed-end moment, and fixed-end shear force, even when using a minimal number of elements.

Bifurcation Buckling Analysis

The Timoshenko beam elements are now being used for the bifurcation buckling analysis of both prismatic and tapered beams. The same fixed-fixed supported beam as in the static analysis, with $L/h_B = 10$, is considered. Additionally, the beam has been modified to have a tapered shape, as illustrated in Figure 3. Two tapering ratios are considered, namely $c = 0.5$ and $c = 0.8$ (refer to Figure 3 for the definition of c).

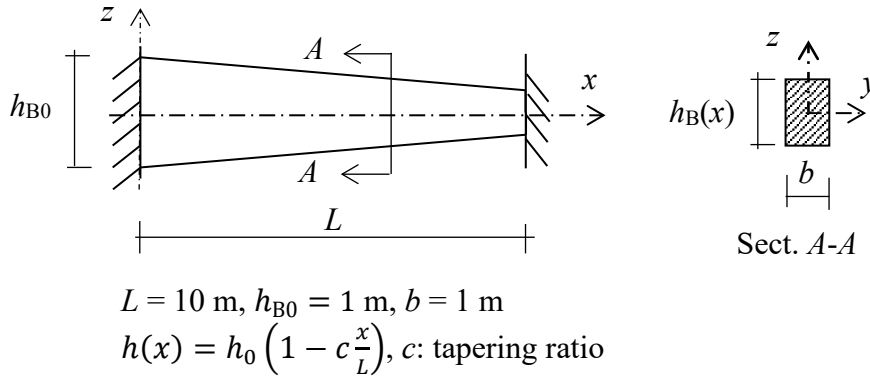


Figure 3. Tapered Fixed-Fixed Supported Beam

The resulting critical buckling loads, normalized to their respective reference values, are presented in Tables 4(a)(c). The reference value for the prismatic beam is calculated using the following analytical formula ([19] as cited in [20]):

$$P_{cr} = \frac{\pi^2 EI_Y}{L_{eff}^2} \left(\frac{1}{1 + \frac{\pi^2 EI_Y}{L_{eff}^2 GA_s}} \right) \tag{45}$$

where the effective buckling length for the fixed-fixed supported beam is $L_{eff} = L/2$. For the tapered beams, since an analytical solution is unavailable, the reference values are obtained from finite element analysis results using 48 cubic LSS-based elements. These values are taken as the reference solution because of the excellent performance of the cubic-LSS-based beam element and additionally, the use of 48 cubic elements represents a very fine finite element model. These reference values are listed in the last row of Table 4(c).

The findings from the static analysis can be applied to the bifurcation buckling analysis. The results converge to their reference values. The performance of the LSS-based elements is superior to that of the original beam elements. The accuracy of both linear and quadratic LSS-based elements is the same as that of the corresponding elements with the DSG technique, while the cubic elements show a slight discrepancy in accuracy.

Free Vibration Analysis

The LSS-based Timoshenko beam elements are utilized to determine the first eight free-vibration frequencies of a tapered fixed-fixed supported beam of $L/h_B = 10$ with the tapering ratio of $c = 0.5$, which has been considered in the bifurcation buckling analysis. The mass density is taken as $\rho = 1000 \text{ kg/m}^3$. The analysis is conducted using 16 beam elements. As in the bifurcation buckling analysis, the natural frequencies (in the unit of Hz) obtained with 48 elements of the cubic LSS-based beam element are used as the reference solution because of the unavailability of analytical results. The results are listed in Table 5.

The table demonstrates the superiority of the field-consistent LSS-based beam elements compared to the original inconsistent beam elements when predicting natural frequencies, particularly for linear and quadratic beam elements. As expected, higher-order beam elements provide greater accuracy than the lower-order elements. Consistent with the findings in static and buckling analyses, the results for the linear and quadratic LSS-based and DSG beam elements are identical, while those for the cubic beam elements show slight differences.

Table 4. Normalized Critical Buckling Loads of the Prismatic ($C = 0$) and Taped Fixed-Fixed Supported Beams of $L/H_b = 10$ for Different Numbers of Elements, N_e , Obtained using Different Beam Elements

(a) Normalized Results using Linear Beam Elements

N_{el}	Tapering ratio = 0		Tapering ratio = 0.5		Tapering ratio = 0.8	
	LSS SF & DSG	Original SF	LSS SF & DSG	Original SF	LSS SF & DSG	Original SF
4	1.5340	3.6276	1.7928	6.2890	3.2500	14.6035
8	1.1012	1.5822	1.1498	2.2133	1.4583	4.4319
16	1.0238	1.1409	1.0354	1.3048	1.1143	1.9873
32	1.0059	1.0349	1.0087	1.0770	1.0288	1.2840

(b) Normalized Results using Quadratic Beam Elements

N_{el}	Tapering ratio = 0		Tapering ratio = 0.5		Tapering ratio = 0.8	
	LSS SF & DSG	Original SF	LSS SF & DSG	Original SF	LSS SF & DSG	Original SF
4	1.0137	1.0613	1.0269	1.1671	1.2272	1.8825
8	1.0009	1.0051	1.0021	1.0166	1.0214	1.1471
16	1.0001	1.0003	1.0001	1.0013	1.0016	1.0179
32	1.0000	1.0000	1.0000	1.0001	1.0001	1.0015

(c) Normalized Results using Cubic Beam Elements and the Exact Critical Buckling Loads

N_{el}	Tapering ratio = 0			Tapering ratio = 0.5			Tapering ratio = 0.8		
	LSS SF	DSG	Original SF	LSS SF	DSG	Original SF	LSS SF	DSG	Original SF
4	1.0002	0.9986	1.0013	1.0011	1.0002	1.0026	1.0182	1.0143	1.1072
8	1.0000	0.9999	1.0000	1.0000	0.9998	1.0001	1.0005	1.0012	1.0037
16	1.0000	1.0000	1.0000	1.0000	1.0000	1.0000	1.0000	1.0000	1.0001
32	1.0000	1.0000	1.0000	1.0000	1.0000	1.0000	1.0000	1.0000	1.0000
P_{cr} exact	2.9890.E+05 kN			1.1344.E+05 kN					

Table 5. The First Eight Natural Frequencies of the Taped Fixed-Fixed Supported Beams of $L/H_b = 10$, which are Obtained using 16 Beam Elements of Different Formulations, Normalized to the Reference Frequencies

Mode shape	Reference frequency* (Hz)	Normalized natural frequency						
		Linear element		Quadratic element			Cubic	
		LSS SF & DSG	Original SF	LSS SF & DSG	Original SF	LSS SF	DSG	Original SF
1	22.9107	1.0138	1.1268	1.0000	1.0007	1.0000	1.0000	1.0000
2	60.4541	1.0325	1.1379	1.0001	1.0012	1.0000	1.0000	1.0000
3	112.557	1.0572	1.1540	1.0004	1.0020	1.0000	1.0000	1.0000
4	175.709	1.0872	1.1750	1.0011	1.0031	1.0000	0.9999	1.0000
5	247.187	1.1214	1.2003	1.0021	1.0046	1.0000	0.9999	1.0000
6	324.862	1.1595	1.2298	1.0037	1.0066	1.0000	0.9998	1.0001
7	407.154	1.2008	1.2629	1.0060	1.0093	1.0001	0.9997	1.0001
8	492.898	1.2448	1.2989	1.0091	1.0126	1.0002	0.9996	1.0002

*Obtained using 48 elements of the cubic LSS SF element

Remarks

All the examples presented are based on the presumption that the interior element nodes are located at their ‘natural’ positions in the Cartesian coordinate system. For a quadratic beam element, this means the nodes are at the mid-points, while for a cubic beam element, they are at the one-third points. If the interior element nodes do not lay at these natural positions, the use of the LSS shape functions cannot provide a consistent shear strain field distribution, leading to very poor results (shear locking). Prathap and Naganarayana [17] proposed a method to modify the use of the LSS shape functions for a quadratic Timoshenko beam element so that it can maintain the shear strain field consistency.

CONCLUSIONS

The variational foundation for the redistribution of shear strain in Timoshenko beam elements has been presented. This theoretical groundwork leads to a systematic procedure for deriving LSS shape functions. The LSS shape functions for linear, quadratic, and cubic Timoshenko beam elements have been derived and are expressed explicitly. These shape functions ensure field consistency within the beam elements.

The LSS-based Timoshenko beam elements were applied to linear static analysis, bifurcation buckling analysis, and free vibration analysis of prismatic and tapered beams. The numerical tests demonstrated that the LSS-based beam

elements are free from shear locking and yield accurate and reliable results. Their performance is practically the same as that of the consistent beam elements with the DSG technique; however, the implementation for the LSS shape functions is simpler than that of the DSG technique.

Further research could explore the development of LSS shape functions for plate and shell finite elements. Additionally, the potential application of the LSS approach to enhanced finite element methods, such as isogeometric analysis and Kriging-based FEM, warrants investigation.

REFERENCES

1. Han, S.M., Benaroya, H., and Wei, T., Dynamics of Transversely Vibrating Beams using Four Engineering Theories, *Journal of Sound and Vibration*, Elsevier, 225(5), 1999, pp. 935–988, doi: 10.1006/JSVI.1999.2257.
2. Hughes, T.J.R., Taylor, R.L., and Kanok-Nukulchai, W., A Simple and Efficient Finite Element for Plate Bending, *International Journal for Numerical Methods in Engineering*, Wiley, 11(10), 1977, pp. 1529–1543, doi: 10.1002/nme.1620111005.
3. Prathap, G., The Displacement-Type Finite Element Approach— From Art to Science, *Progress in Aerospace Sciences*, Elsevier, 30(4), 1994, pp. 295–405, doi: 10.1016/0376-0421(94)90007-8.
4. Prathap, G., *The Finite Element Method in Structural Mechanics*, Springer, 1993.
5. Wong, F.T. and Syamsoeyadi, H., Kriging-based Timoshenko Beam Element for Static and Free Vibration Analyses, *Civil Engineering Dimension*, 13(1), 2011, pp. 42–49, doi: 10.9744/ced.13.1.42-49.
6. Bouclier, R., Elguedj, T., and Combescure, A., Locking Free Isogeometric Formulations of Curved Thick Beams, *Computer Methods in Applied Mechanics and Engineering*, Elsevier, 245–246, 2012, pp. 144–162, doi: 10.1016/j.cma.2012.06.008.
7. Bletzinger, K.U., Bischoff, M., and Ramm, E., A Unified Approach for Shear-Locking-Free Triangular and Rectangular Shell Finite Elements, *Computers and Structures*, Elsevier, 75(3), 2000, pp. 321–334, doi: 10.1016/S0045-7949(99)00140-6.
8. Wong F.T. and Sugianto, S., Study of the Discrete Shear Gap Technique in Timoshenko Beam Elements, *Civil Engineering Dimension*, 19(1), 2017, pp. 54–62, doi: 10.9744/CED.19.1.54-62.
9. Wong, F.T., Sulistio, A., and Syamsoeyadi, H., Kriging-based Timoshenko Beam Elements with the Discrete Shear Gap Technique, *International Journal of Computational Methods*, World Scientific, 15(7), 2018, pp. 1850064-1–27, doi: 10.1142/S0219876218500640.
10. Wong, F.T., Tanoyo, N., and Gosaria, T.C., Free-Vibration and Buckling Analyses of Beams using Kriging-Based Timoshenko Beam Elements with the Discrete Shear Gap Technique, *Civil Engineering Dimension*, 26(1), 2024, pp. 21–31, doi: 10.9744/ced.26.1.21-31.
11. Wong, F.T., Santoso, S.W., and Sutrisno, M., Locking-free Kriging-based Timoshenko Beam Elements using an Improved Implementation of the Discrete Shear Gap Technique, *Civil Engineering Dimension*, 24(1), 2022, pp. 11–18, doi: 10.9744/ced.24.1.11-18.
12. Wong, F.T. and Gunawan, J., Locking-Free Kriging-Based Curved Beam Elements with the Discrete Strain Gap Technique, *International Journal of Computational Methods*, World Scientific, 21(9), 2024, pp. 2450033-1–38, doi: 10.1142/s0219876224500336.
13. Echter, R. and Bischoff, M., Numerical Efficiency, Locking and Unlocking of NURBS Finite Elements, *Computer Methods in Applied Mechanics and Engineering*, Elsevier, 199(5–8), 2010, pp. 374–382, doi: 10.1016/j.cma.2009.02.035.
14. Prathap, G. and Babu, C.R., An Isoparametric Quadratic Thick Curved Beam Element, *International Journal for Numerical Methods in Engineering*, Wiley, 23(9), 1986, pp. 1583–1600, doi: 10.1002/nme.1620230902.
15. Babu, C.R. and Prathap, G., A Linear Thick Curved Beam Element, *International Journal for Numerical Methods in Engineering*, Wiley, 23(7), 1986, pp. 1313–1328, doi: 10.1002/nme.1620230709.
16. Prathap, G. and Babu, C.R., Field-Consistent Strain Interpolations for the Quadratic Shear Flexible Beam Element, *International Journal for Numerical Methods in Engineering*, Wiley, 23(11), 1986, pp. 1973–1984, doi: 10.1002/nme.1620231102.
17. Prathap, G. and Naganarayana, B.P., Field-Consistency Rules for a Three-Noded Shear Flexible Beam Element under Non-Uniform Isoparametric Mapping, *International Journal for Numerical Methods in Engineering*, Wiley, 33(03), 1992, pp. 649–664, doi: 10.1002/nme.1620330310.
18. Cowper, G.R., The Shear Coefficient in Timoshenko's Beam Theory, *ASME, Journal of Applied Mechanics*, 33(2), 1966, pp. 335–340, doi: 10.1115/1.3625046.
19. Bažant, Z.P. and Cedolin, L., *Stability of Structures: Elastic, Inelastic, Fracture, and Damage Theories*, Dover, New York, 1991.
20. Kosmatka, J.B., An Improved Two-Node Finite Element for Stability and Natural Frequencies of Axial-Loaded Timoshenko Beams, *Computer and Structures*, Elsevier, 57(1), 1995, pp. 141–149, doi: 10.1016/0045-7949(94)00595-T.